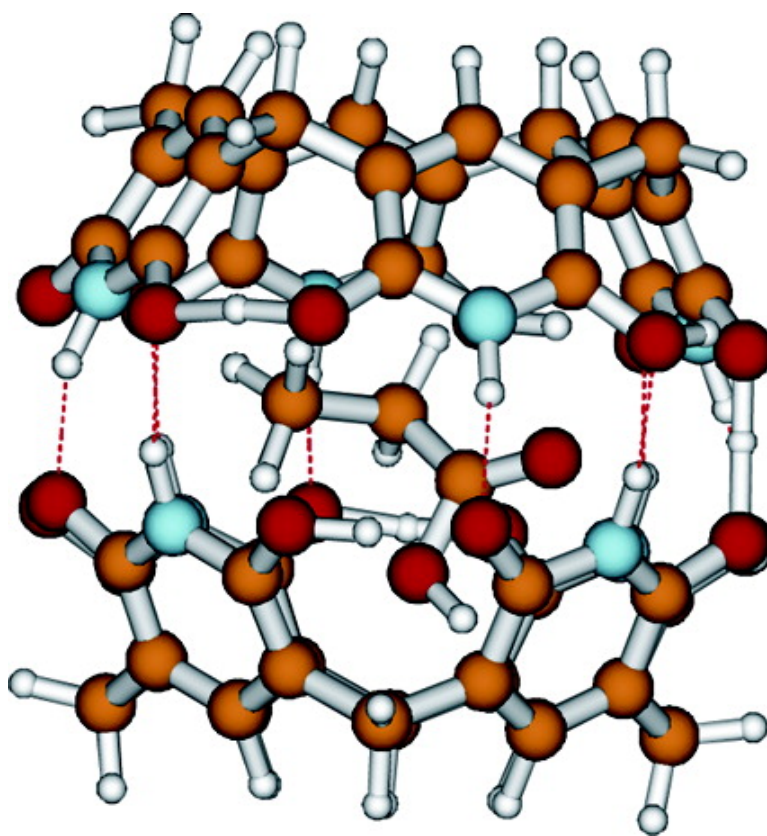Article

Encapsulated Guest Molecules in the Dimer of Octahydroxypyridine[4]arene

Matthias C. Letzel, Bjrn Decker, Alexander B. Rozhenko, Wolfgang W. Schoeller, and Jochen Mattay

More About This Article

Additional resources and features associated with this article are available within the HTML version:

- Supporting Information
- Links to the 2 articles that cite this article, as of the time of this article download
- Access to high resolution figures
- Links to articles and content related to this article
- Copyright permission to reproduce figures and/or text from this article

Encapsulated Guest Molecules in the Dimer of Octahydroxypyridine[4]arene

Matthias C. Letzel, Björn Decker, Alexander B. Rozhenko,
Wolfgang W. Schoeller, and Jochen Mattay*

*Contribution from the Fakultät für Chemie, Universität Bielefeld,
Postfach 100131, 33501 Bielefeld, Germany*

Received February 17, 2004; E-mail: mattay@uni-bielefeld.de

Abstract: Recently a new type of calix[4]arenes has been synthesized via condensation of 2,6-dihydroxypyridine and a number of aldehydes. This type of pyridine[4]arenes forms capsules consisting of two single pyridine[4]arenes. These capsules can incorporate different guest molecules, like carboxylic acids and amides in this case. We proved that the guest acids really are incorporated inside the cavity of the capsules by electrospray mass spectrometry, NMR spectroscopy, and theoretical calculations.

Introduction

2,6,8,12,14,18,20,24-Octahydroxypyridine[4]arenes were first synthesized in our group by direct acidic condensation of 2,6-dihydroxypyridine with several aliphatic and aromatic aldehydes.[1] Pyridine containing calixarenes have been prepared before using alternative multistep pathways.[2−4] But these calixarenes feature neither hydroxy groups nor substituents at the stereogenic methine center. The substitution pattern of our 2,6,8,12,14,18,20,24-octahydroxypyridine[4]arenes is expected to promote self-organization processes comparable to those of uracil derivatives if complementary molecules are present. In addition new host−guest complexes may be available by complexation of metal cations and anions as well. Both fields of research are currently under investigation.[5−8]

As the very first example of a hydrogen-bonded capsule, Rebeks so-called tennis ball was reported in 1993.[9] In the following years calixarenes and modified calixarene systems attracted great interest concerning their aggregation and self-assembling behavior. This interest is based on their easy generation, multiple modification facilities, and rigidity. Numerous hydrogen-bonded capsules have been reported in recent years.[10,11] Calixarenes based on self-complementary glycoluril building blocks,[12] urea functions,[13,14] and imide-bridged[15] or C_{2v}-symmetric derived resorcarenes[16] show the formation of dimeric structures. Alanine-functionalized calix[4]arenes dimerize even

in polar, protic solvents.[17] With suitable guests, unsubstituted resorc[4]arenes show the formation of dimeric[18] but also hexameric[5,19,20] molecular containers. Due to their structural features, resorc[4]arenes play an important role as host molecules for a variety of neutral and charged guest compounds.

Since its invention electrospray ionization (ESI) became the most powerful tool in mass spectrometry for the examination of charged host−guest compounds. By desolvating ions from solution it is expected that most of the analyte structural features are transferred into the gas-phase giving a close approximation to the solution state.

So far, ESI−MS has mainly been used in calixarene chemistry simply as an analytical method to control the result of a synthetic procedure. To our knowledge only a few investigations have been undertaken concerning the analysis of host−guest complexes with calixarenes using ESI−MS; among them are binding selectivities of alkali metal ions,[21−23] gas-phase inclusion of

(1) Gerkensmeier, T.; Näther, C.; Mattay, J. *Chem. Eur. J.* **2001**, *7*, 465−474.
(2) Newcome, G. R.; Joo, J. Y.; Frontzek, F. R. *J. Chem. Soc., Chem. Commun.* **1987**, 854−856.
(3) Kral, V.; Gale, P. A.; Anzenbacher, P.; Jursikova, K.; Lynch, V.; Sessler, J. L. *J. Chem. Soc., Chem. Commun.* **1998**, 9−10.
(4) Kral, V.; Sessler, J. L.; Volf, P. A.; Volf, R.; Shishkanova, T. V. *J. Am. Chem. Soc.* **1999**, *121*, 8771−8775.
(5) Gerkensmeier, T.; Agena, C.; Iwanek, W.; Fröhlich, R.; Kotila, S.; Näther, C.; Mattay, J. *Eur. J. Org. Chem.* **1999**, 2257−2262.
(6) Agena, C.; Wolff, C.; Mattay, J. *Eur. J. Org. Chem.* **2001**, *15*, 2977−2981.
(7) Letzel, M. C.; Agena, C.; Mattay, J. *Eur. J. Mass Spectrom.* **2001**, *7*, 35−38.
(8) Letzel, M. C.; Agena, C.; Mattay, J. *J. Mass Spectrom.* **2002**, *37*, 63−68.
(9) Wyler, R.; de Mendoza, J.; Rebek, J. *Angew. Chem.* **1993**, *105*, 1820−1821; *Angew. Chem., Int. Ed. Engl.* **1993**, *32*, 1699−1701.

(10) Rebek, J. *Chem. Commun.* **2000**, 637−643. Vysotsky, M. O.; Böhmer, V. *Aust. J. Chem.* **2001**, *54*, 671−677.
(11) Hof, F.; Craig, S. L.; Nuckolls, C.; Rebek, J., Jr. *Angew. Chem.* **2002**, *114*, 1556−1578; *Angew. Chem., Int. Ed.* **2002**, *41*, 1488−1508 and references therein.
(12) O'Leary, B. M.; Szabo, T.; Svenstrup, N.; Schalley, C. A.; Lützen, A.; Schäfer, M.; Rebek, J. *J. Am. Chem. Soc.* **2001**, *123*, 11519−11533.
(13) Mogck, O.; Böhmer, V.; Vogt, W. *Tetrahedron* **1996**, *52*, 8489−8496. Frish, L.; Vysotsky, M. O.; Matthews, S. E.; Böhmer, V.; Cohen, Y. *J. Chem. Soc., Perkin Trans. 2*, **2002**, 88−93.
(14) Scheerder, J.; van Duynhoven, J. P. M.; Engbersen, J. F. J.; Reinhoudt, D. N. *Angew. Chem.* **1996**, *108*, 1172−1175; *Angew. Chem., Int. Ed. Engl.* **1996**, *35*, 1090−1093.
(15) Heinz, T.; Rudkevich, D. M.; Rebek, J. *Nature* **1998**, *394*, 764−766.
(16) Shivanyuk, A.; Paulus, E.; Böhmer, V. *Angew. Chem.* **1999**, *111*, 3091−3094.
(17) Brewster, R. E.; Shuker, S. B. *J. Am. Chem. Soc.* **2002**, *124*, 7902−7903.
(18) Murayama, K.; Aoki, K. *Chem. Commun.* **1998**, 607−608. Shivanyuk, A.; Rebek, J. *Chem. Commun.* **2001**, 2374−2375.
(19) Shivanyuk, A.; Rebek, J. *Proc. Natl. Acad. Sci. U.S.A.* **2001**, *98*, 7662−7665.
(20) McGillivray, R. L.; Atwood, J. L. *Nature* **1997**, *389*, 469−472.
(21) Blanda, M. T.; Farmer, D. B.; Brodbelt, J. S.; Goolsby, B. J. *J. Am. Chem. Soc.* **2000**, *122*, 1486−1491.
(22) Goolsby, B. J.; Brodbelt, J. S.; Adou, E.; Blanda, M. *Int. J. Mass Spectrom.* **1999**, *193*, 197−204.
(23) Allain, F.; Virelizier, H.; Moulin, C.; Jankowski, C. K.; Dozol, J. F.; Tabet, J. C. *Spectroscopy* **2000**, *14*, 127−139.
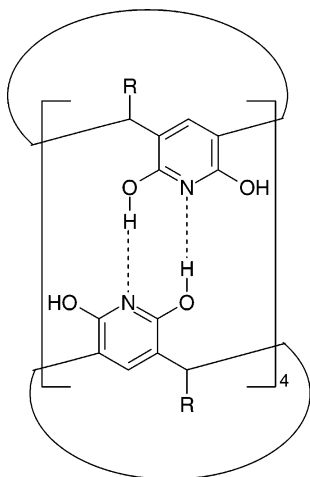
Figure 1. Pyridine[4]arene dimer [C·C] (with R = C₁₁H₂₃) and [C′·C′] (with R = H for calculated structures, Table 2).
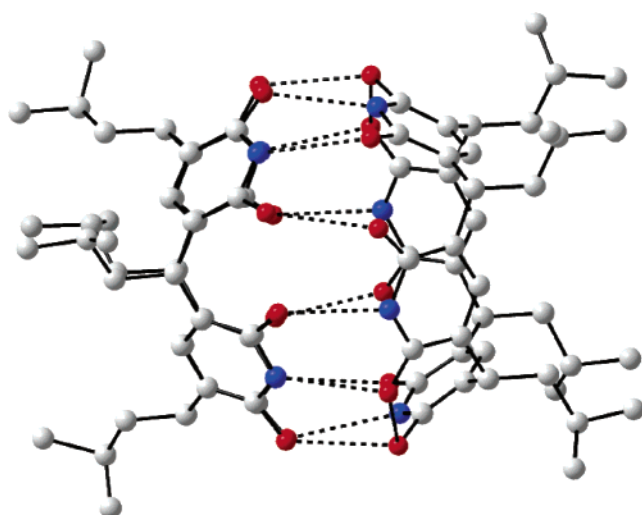

Figure 2. Dimer of octacydroxy-tetra-*iso*-butyl-pyridine[4]arene in the crystal structure.

neutral molecules,[24] and inclusion of alkylammonium ions in calixarene capsules.[25-27]

Results and Discussion

Mass Spectrometry. Calix[4]arenes, like the one shown in Figure 1 (always called calixarene **C** in the following text), form stable dimers in the crystal structure (X-ray) as well as under electrospray conditions in the mass spectrometer. The crystal structure of the pyridine[4]arenes shows head−head dimers attracted by hydrogen bonding (Figure 2). These dimers form a cavity which may include molecules or ions if the guest fits into the cavity. This kind of guest incorporation can be observed in the ESI FT-ICR mass spectra (Figure 3). Other than the most abundant pseudomolecular ion [C + H]⁺, the gas-phase dimer [C·C + H]⁺ of the calixarene **C** is observed. The addition of small amounts of different carboxylic acids (Table 1) results in a partial incorporation of those acids into the cavity of the dimer,
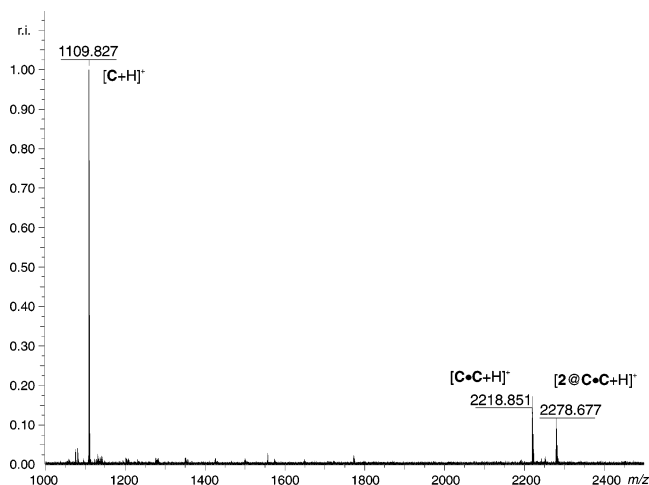
(24) Nuutinen, J. M. J.; Irico, A.; Vincenti, M.; Dalcanale, E.; Pakarinen, J. M. H.; Vainiotalo, P. *J. Am. Chem. Soc.* **2000**, *122*, 10090−10100.
(25) Schalley, C. A.; Castellano, R. K.; Brody M. S.; Rudkevich, D. M.; Siuzdak, G.; Rebek, J., Jr. *J. Am. Chem. Soc.* **1999**, *121*, 4568−4579.
(26) Lippmann, T.; Wilde, H.; Pink, M.; Schäfer, A.; Hesse, M.; Mann, G. *Angew. Chem., Int. Ed. Engl.* **1993**, *32*, 1195−1197.
(27) Mansikkamäki, H.; Nissinen, M.; Schalley, C. A.; Rissanen, K. *New J. Chem.* **2003**, *27*, 88−97.

Figure 3. FT-ICR-MS (ESI) mass spectrum of pyridine[4]arene (**C**) with addition of 0.2% acetic acid (**2**).
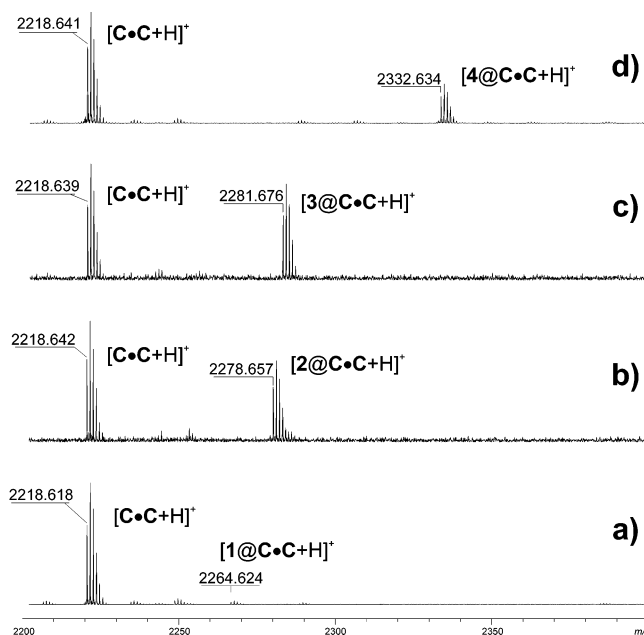

Figure 4. FT-ICR-MS (ESI) mass spectrum of dimer region with pyridine-[4]arene (**C**) and different carboxylic acids (a) formic acid (**1**), (b) acetic acid (**2**), (c) *d*₃-acetic acid (**3**), and (d) trifluoroacetic acid (**4**).

as seen in Figures 3 and 4b for acetic acid, to yield [**2**@C·C + H]⁺. No adduct formation like [**2**@C + H]⁺ is observed with the monomeric species. We assume that the monomeric calix-arene acid complex might not be stable enough to survive the ionization process intact. Therefore we assume that in the dimer the acid molecule is incorporated inside the calixarene cavity. If it were placed outside the cavity, we cannot see any reason this kind of complex should ride out the ionization process other than the monomer. When using homologous carboxylic acids of different size (Table 1), it turns out that there is only room for small variations: we also find incorporation of guests such as formic acid (**1**) (Figure 4a, very poor signal), *d*₄-acetic acid (**3**) (Figure 4c), trifluoro acetic acid (**4**) (Figure 4d), and propionic acid (**5**) (Figure 5e). Acids that are more bulky than propionic acid are not incorporated in the capsule anymore (Figure 5f−h). It can be observed that on higher acid concentra-tions the abundance of the dimer decreases or cannot be observed at all. This can be traced back to the fact that the acids are breaking the dimer's hydrogen bonds, cracking the dimers
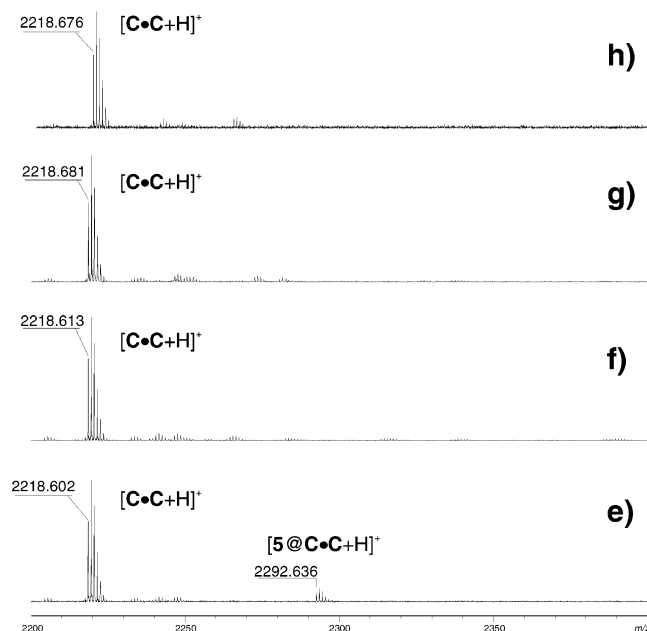
Figure 5. FT-ICR-MS (ESI) mass spectrum of dimer region with pyridine-[4]arene (**C**) and different carboxylic acids (e) propionic acid (**5**), (f) butyric acid (**6**), (g) 2-methyl butyric acid (**7**), and (h) 2,2-dimethyl butyric acid (**8**).
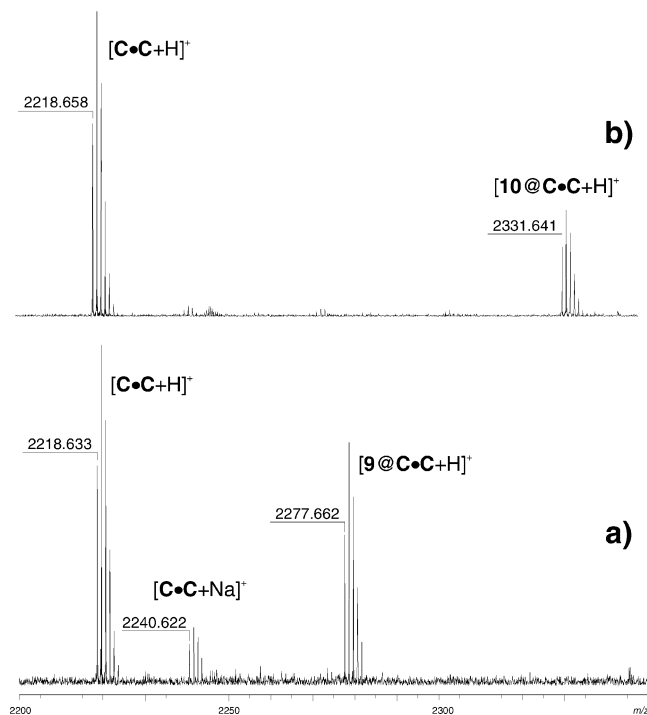

Figure 6. FT-ICR-MS (ESI) mass spectrum of dimer region with pyridine-[4]arene (**C**) and different carboxylic acid amides (a) acetamide (**9**) and (b) trifluoroacetamide (**10**). The signal in spectrum (a) at *m/z* 2240.622 is the corresponding $[\mathbf{C} + Na]^+$ ion. Interestingly no sodium adduct is observed for the host−guest complex.
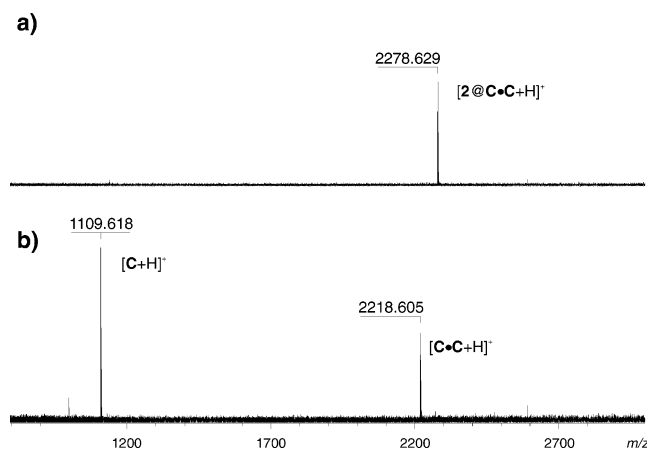

Figure 7. IRMPD experiment with acetic acid encapsulated in the dimer's cavity $[\mathbf{2@C\cdot C} + H]^+$: (a) isolated $[\mathbf{2@C\cdot C} + H]^+$ ion; (b) after IR irradiation (0.1 s): decomposition of the complex into the dimer $[\mathbf{C\cdot C} + H]^+$ without guest and the monomer $[\mathbf{C} + H]^+$ is observed.

Table 1. Guest Molecules Used in Complexation Experiments

no.	guest	no.	guest
1	$HCOOH$	**6**	$CH_3(CH_2)_2-COOH$
2	CH_3-COOH	**7**	$CH_3-CH_2-CH(CH_3)-COOH$
3	CD_3-COOH	**8**	$CH_3-CH_2-C(CH_3)_2-COOH$
4	CF_3-COOH	**9**	CH_3-CONH_2
5	CH_3-CH_2-COOH	**10**	CF_3-CONH_2

to monomers. This effect is also observed by ^{19}F NMR spectroscopy.

So far we observed host−guest complexes with simple carboxylic acids in the ESI−MS. Therefore we first extended our investigation to a homologous row of different carboxylic acids to get an idea of the size limits of the cavity. Because of the problems arising from competition with the hydrogen bonding of the complex, as observed in the TFA NMR experiments (Figure 11), we also checked some amides (Table 1), which also were complexed quite well under ESI−MS conditions. Those amides were acetamide (**9**) (Figure 6a) and trifluoroacetamide (**10**) (Figure 6b), which were successfully incorporated. In Figure 6a beside the protonated dimer $[\mathbf{C\cdot C} + H]^+$ at *m/z* 2218.6, also the sodiated dimer $[\mathbf{C\cdot C} + Na]^+$ at *m/z* 2240.6 is observed. For the host−guest complex $[\mathbf{9@C\cdot C}+H]^+$, no corresponding sodiated species was detected. In our opinion the cavity of the sodiated dimer $[\mathbf{C\cdot C} + Na]^+$ is blocked by the sodium ion leaving no room for other guest molecules (Table 1). On the other hand the small proton might be located somewhere on one of the nitrogen atoms of the calixarene and is not able to block the cavity.

An MS/MS experiment with the complex $[\mathbf{2@C\cdot C} + H]^+$ using excitation by infrared irradiation (IRMPD) was performed. Prior to the infrared irradiation, the parent ion $[\mathbf{2@C\cdot C} + H]^+$ was isolated using a correlated sweep (Figure 7a). Infrared laser irradiation yields the monomeric fragment ion $[\mathbf{C} + H]^+$ and some dimer ion $[\mathbf{C\cdot C} + H]^+$ by loss of the guest (Figure 7b). This experiment supports our hypothesis that the complex of carboxylic acid and the monomeric pyridine[4]arene is not very stable and dissociates quickly after cleavage of the dimer complex. This might also be the case for a complex where the carboxylic acid is attached outside the dimer's cavity as an ion molecule complex for a short time after irradiation.

We also performed some IRMPD experiments on $[\mathbf{10@C\cdot C} + H]^+$ with the same results as observed for $[\mathbf{2@C\cdot C} + H]^+$ (data not shown). Furthermore we were able to tune the laser

intensity in such a way that the capsule releases the guest **10** without further fragmentation to the monomer.

In summary of these results, the cavity of the pyridinearene capsule appears to be quite small, so that it is difficult to find other guest molecules that are not too volatile and fulfill the constraints given by the size of the cavity.
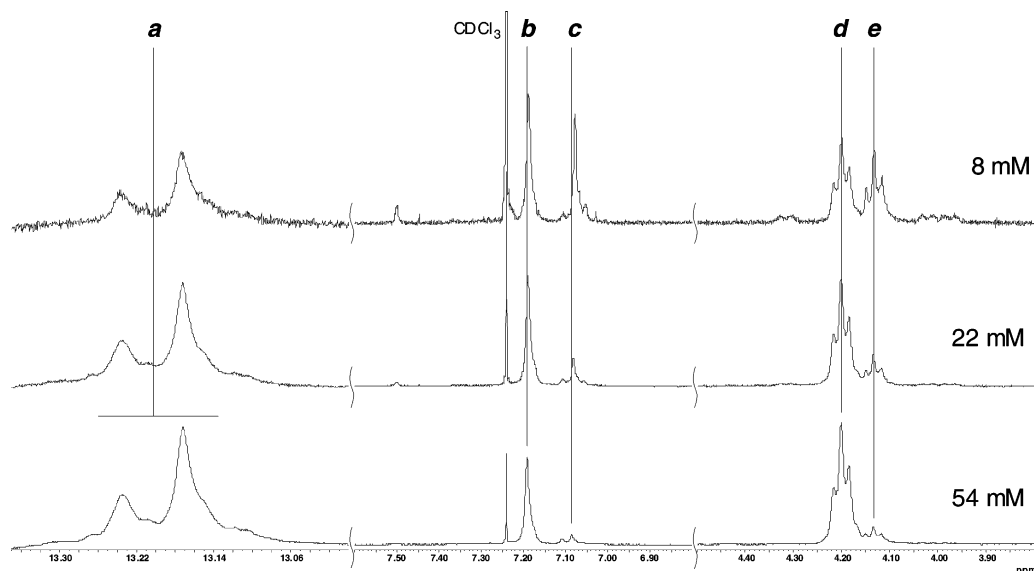
Figure 8. ¹H NMR of the pyridine[4]arene in three different concentrations of 8, 22, and 54 mM in CDCl₃. Dimer signals are marked with **a** (H-bonding), **b** (aromatic proton), and **d** (methine proton). Monomer signals are marked with **c** (aromatic proton) and **e** (methine proton).
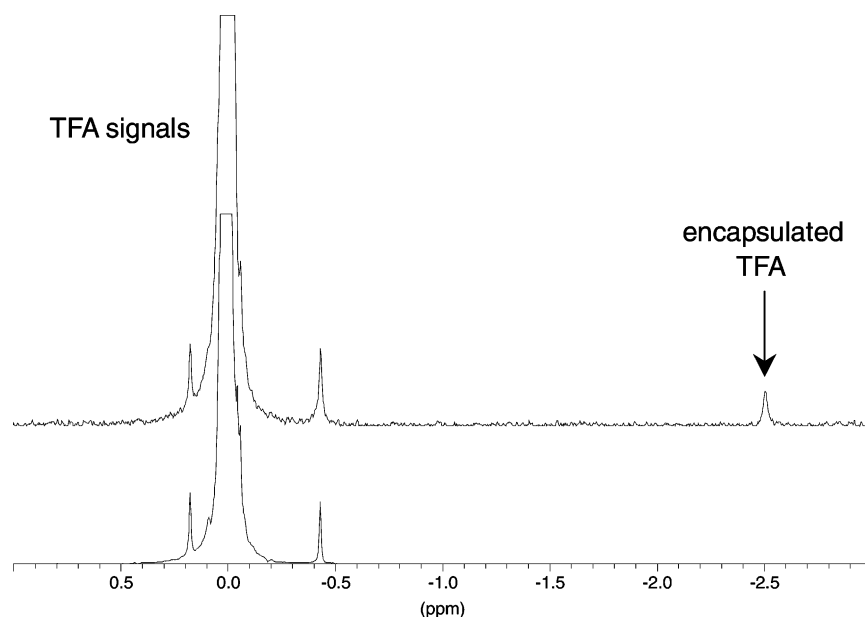

Figure 9. ¹⁹F NMR spectrum of pyridine[4]arene (**C**) (46mM) with 30 (upper spectrum) and 160 mM (lower spectrum) TFA.

NMR Spectroscopy. The dimerization of pyridine[4]arenes can be followed by ¹H and ¹³C NMR spectroscopy. At high concentrations (100 mM), only one set of signals is observed corresponding to the dimeric pyridine[4]arene. The ¹H spectrum shows a singlet at 7.19 ppm for the aromatic protons (Figure 8, **b**) and a triplet at 4.20 ppm for the methine protons (Figure 8, **d**). The existence of H-bonding can be documented by a low-field signal at 13.1 ppm to 13.4 ppm (Figure 8, **a**) and another broad signal from 8.50 to 11.0 ppm.

The ¹³C spectrum shows only one set of signals for a C_4-symmetric species. These results indicate a dimeric structure built up by two pyridine[4]arenes twisted by 30° (Figure 1). The structure is already known from the crystal structure of the tetra-*iso*-butylpyridine[4]arene (Figure 2).[1]

With decreasing concentration, new sets of ¹H and ¹³C signals arise for the monomeric species (Figure 8). The ¹H spectrum shows two high field shifted signals for the aromatic protons (Figure 8, **c**) at 7.08 ppm and at 4.13 ppm for the methine

protons (Figure 8, **e**). The low field shifted dimer signals disappear with decreasing concentration. Hydroxy protons that are involved in H-bonding cannot be detected anymore. The ¹³C spectrum shows a change of symmetry from C_4 to C_{4v}, indicating the existence of a monomer with perfect *crown* conformation. The same effect can be achieved by addition of polar additives to a highly concentrated solution of the pyridine-[4]arene.

The association constant for the formation of dimeric pyridine[4]arenes was determined by ¹H NMR spectroscopy, since the signals for the monomeric and dimeric species are separated and their actual concentrations could be calculated by direct integration (Figure 8).[28] Concentration-dependent measurements yield an association constant $k_a = 146 \pm 8$ M^{-1} in chloroform. ¹H NMR investigations in CHCl₃/CDCl₃ give no indication for encapsulated chloroform molecules. Because

(28) Schneider, H.-J.; Yatsimirsky, A. *Principles and Methods in Supramolecular Chemistry*; Wiley: Chichester, 2000.
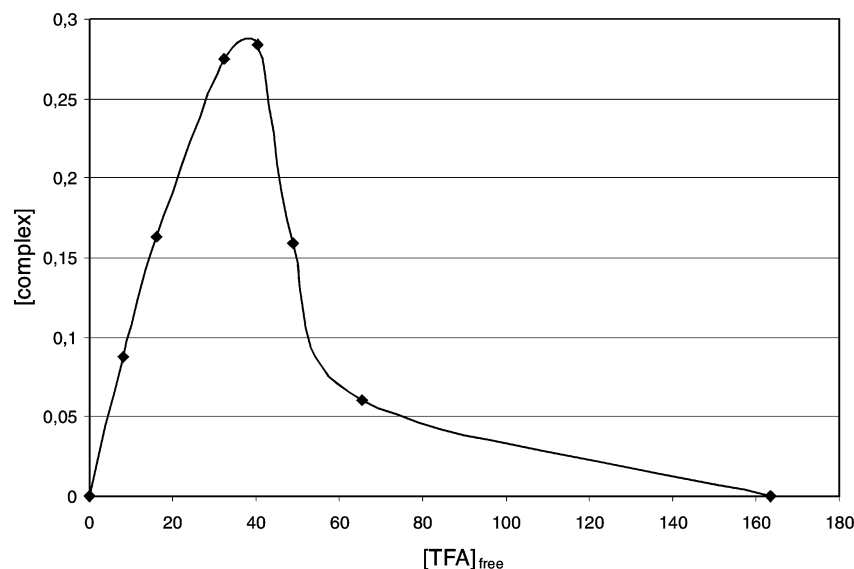
Figure 10. Complex formation (from ^{19}F NMR integration) depending on the TFA concentration.

of its low solubility, the dimerization could not be studied in other solvents such as benzene or dichloromethane.

With further decreasing concentration, numerous new signals come up. These signals cannot be allocated to a certain species but might be the result of the tautomerism of the individual 2,6-dihydroxypyridine units.[29-31]

The complex studies with TFA were recorded at a constant pyridine[4]arene concentration of 46.7 mM in water-saturated deuterated chloroform. The TFA concentration was varied from 0 to 160 mM, and the complexation of TFA was confirmed by ^{19}F NMR spectroscopy at 298 K.

For low TFA concentrations, the spectra exhibit an additional upfielded signal for complexed TFA compared to the spectrum of TFA in CDCl$_3$ showing solely the typical singlet with its satellites (Figure 9). The exchange of TFA is slow compared to the ^{19}F NMR time scale, and consequently the concentration of complexed TFA can be obtained by integration of the measured signals. The complex concentration is low compared to the concentration of free TFA.

For TFA concentrations up to 30 mM, a growing complex concentration is obtained. A maximum is reached for approximately 40 mM of TFA. With further growing acid concentration, the formation of dimers is decreased. In the same way the formation of the complex is reduced (Figure 10).

With higher TFA concentrations of about 150 mM, all dimeric or complex species are destroyed. Only the signal for free TFA can be detected in the ^{19}F spectrum. In the ^{1}H spectrum, the signals for the monomeric pyridine[4]arene (**C**) are observed and none for a dimer.

The ^{1}H spectra exhibit the signals of the monomer and the dimeric species. New signals for the complex are not detected (data not shown). This may be the consequence of their low intensity compared to empty dimer or superposition of the dimer with the complex. Investigations with other complex partners such as ammonium or tropylium cations are still in progress.

VPO Measurements. VPO (Vapor Pressure Osmometry) experiments with the pyridine[4]arene (**C**) in chloroform lead

(29) Katritzky, A. R.; Popp, F. D.; Rowe, J. D. *J. Chem. Soc. B* **1966**, 562–564.
(30) Spinner, E.; White, J. C. B. *J. Chem. Soc. B* **1966**, 991–995.
(31) Spinner, E.; Yeoh, G. B. *Aust. J. Chem.* **1971**, *24*, 2557–2573.

Table 2. Calculated Total Energy Values and ΔE^2 Values Calculated for Model Structures **11**–**20** and Free Acids

structure	complex	total charge[a]	total energy (dimers and complexes with acids), au	total energy (free guests), au	$\Delta E^{2\,b}$, kcal/mol
11	**C'·C'**	0	−3496.009 491		
12	**2@C'·C'**	0	−3725.163 598	−229.154 059	0.0
13	**3@C'·C'**	0	−3764.475 410	−268.479 463	8.5
14	**6@C'·C'**	0	−3803.781 566	−307.803 581	19.8
15	**7@C'·C'**	0	−3882.375 185	−386.448 154	51.7
16	**[C'·C' + H]⁺**	+1	−3496.379 864		
17	**[2@C'·C' + H]⁺**	+1	−3725.548 437	−229.154 059	−9.1
18	**[3@C'·C' + H]⁺**	+1	−3764.858 193	−268.479 463	0.7
19	**[6@C'·C' + H]⁺**	+1	−3804.152 474	−307.803 581	19.4
20	**[7@C'·C' + H]⁺**	+1	−3882.764 320	−386.448 154	40.0

[a] Either the neutral capsules (total charge = 0) or the singly protonated form of the capsules (total charge = +1) were calculated. [b] Calculated at the B3LYP/6-311G**//B3LYP/3-21G* level of approximation without ZPE energy correction.

to an average molecular weight of 2230 ± 92 g/mol. This agrees well with the theoretical mass of 2219 g/mol for the dimer. In THF, VPO measurements result in a lower average mass of 1443 ± 78 g/mol. The more polar solvent should reduce the tendency of the formation of dimeric species. In this case, a mixture of monomers and dimers exists in solution.

Theoretical Calculations. The model structures **11**–**20** (Figure 1, R = H, Table 2) involving the model capsule **11** and its protonated form **16** as well as their aggregates with acids were investigated theoretically (with the GAUSSIAN-98 set of programs,[32] at the DFT (B3LYP[33,34]) level of approximation using the 3-21G* standard Gaussian basis set for geometry optimization and the 6-311G** standard Gaussian basis set for

(32) Frisch, M. J.; Trucks, G. W.; Schlegel, H. B.; Scuseria, G. E.; Robb, M. A.; Cheeseman, J. R.; Zakrzewski, V. G.; Montgomery, J. A.; Stratmann, R. E.; Burant, J. C.; Dapprich, S.; Millam, J. M.; Daniels, A. D.; Kudin, K. N.; Strain, M. C.; Farkas, O.; Tomasi, J.; Barone, V.; Cossi, M.; Cammi, R.; Mennucci, B.; Pornelli, C.; Adamo, C.; Clifford, S.; Ochterski, J.; Petersson, G. A.; Ayala, P. Y.; Cui, Q.; Morokuma, K.; Malick, D. K.; Rabuck, A. D.; Raghavachari, K.; Foresman, J. B.; Cioslowski, J.; Ortiz, J. V.; Stefavov, B. B.; Liu, G.; Liashenko, A.; Piskorz, P.; Komaromi, I.; Gomperts, R.; Martin, R. L.; Fox, D. J.; Keith, T.; Al-Laham, M. A.; Peng, C. Y.; Nanayakkara, A.; Gonzalez, C.; Challacombe, M.; Gill, P. M. W.; Johnson, B. G.; Chem, W.; Wong, M. W.; Andres, J. L.; Head-Gordon, M.; Replogle, E. S.; Pople, J. A. *Gaussian 98*, revision A.1; Gaussian, Inc.: Pittsburgh, PA, 1998.
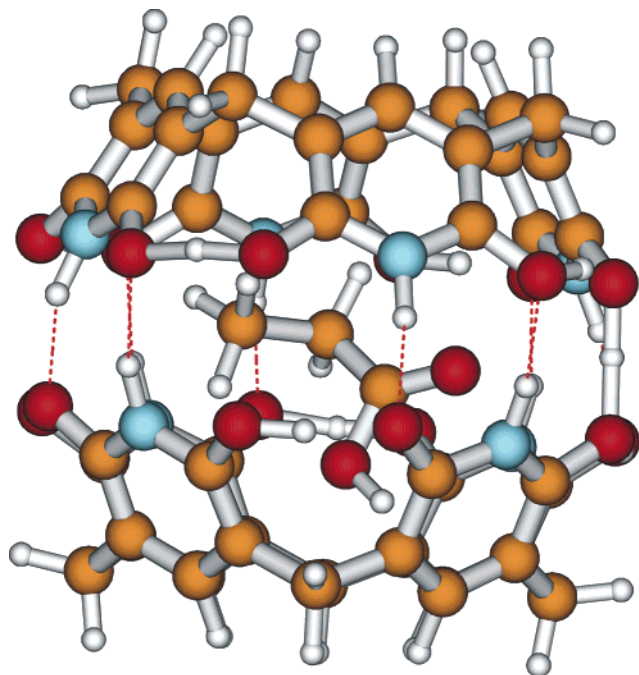
Figure 11. Calculated structure of **3@C′·C′** (Table 2, structure **13**).

the single-point energy calculation). As the calculated capsule structures differ significantly from the species investigated experimentally and due to the relatively low level of approximation by geometry optimization, one could hardly expect a quantitative agreement with the experimental data discussed above. Nevertheless, our calculations predict a high exothermic effect for reaction 1, where the dimer is formed from two pyridine[4]arene molecules.

The encapsulated acid is rigidly fixed and a large number of conformers are feasible. To take care of this aspect, a number of different starting structures were selected which differ by the conformation of the acid molecule, its orientation relative to the aromatic rings, and (in case of the protonated capsules) the protonation sites. All of these varieties were tested until no further lowering of the calculated total energy was achieved. Nevertheless, we cannot completely exclude the existence of other conformations with lower total energies. As we have found, the lowest total energies possess the conformations with the acid molecule lying approximately between the two pyridine-[4]arene cavities. An increase of the alkyl substituent's size forces the alkyl chain of the guest molecule to be twisted still lying in this restricted volume of the cavity (see for example structure **13**, Figure 11). The electronegative oxygen atoms are oriented between the electron-rich pyridine rings.

$$2 \: \mathbf{C'} \rightarrow \mathbf{C' \cdot C'} - 32.8 \: \text{kcal} \qquad (1)$$

As one can see from Table 2, a formation of the host−guest aggregates (reaction 2) seems to be only possible for acetic acid

(33) Becke, A. D. *J. Chem. Phys.* **1993**, *98*, 5648−5652.
(34) Lee, C.; Yang, W.; Parr, R. G. *Phys. Rev.* **1988**, *B37*, 785−789.

and propionic acid in the presence of acid (structures **17**, **18**). Interestingly, the single protonation of the capsule (structure **16**) makes the acid coordination more favorable by 9−12 kcal/mol.

$$\mathbf{C' \cdot C'} + \text{guest} \rightarrow \text{guest@} \mathbf{C' \cdot C'} + \Delta E^2 \qquad (2)$$

Thus, the results of our calculations agree well with the conclusions made on the basis of the experimental FT-ICR MS data.

Experimental Section

Preparation of Octahydroxypyridine[4]arene C. Octahydroxy-pyridine[4]arene **C** was prepared according to the procedure given in the literature.[1]

FT-ICR Mass Spectrometry (ESI). Mass spectra were measured on a Bruker APEX III FT-MS (7T magnet) instrument with the Apollo ESI source. A solution of pyridine[4]arene (**C**) in chloroform (20 μL, 2 nmol/μL) was added to a 0.2% solution of the acid in MeOH/CHCl$_3$ (1:1). In the case of the amides, the given amount of **C** was added to a solution with an amide concentration of 700 pmol/μL. This mixture was introduced into the ESI source by syringe injection with a flow rate of 120 μL/h. Spectra displayed here are the result of summing up to about 100 single measurements.

NMR Spectroscopy. NMR spectra were measured on a Bruker DRX 500. CDCl$_3$ (with the residual CHCl$_3$) was used as internal standard for ^{1}H and ^{13}C spectra. ^{19}F spectra are referenced to TFA. CDCl$_3$ for complexation experiments was saturated with water before use.

Vapor Pressure Osmometry (VPO). Vapor pressure osmometry was performed with a Gonotec Osmomat 070-SA with benzil as calibration standard. Measurements with *rccc*-octa-*O*-acetyl-tetra-*n*-undecyl-resorc[4]arene were carried out in order to confirm the accuracy of the benzil calibration. Measurements in CHCl$_3$ were carried out at 35 °C, in THF at 45 °C. Solvents were tempered for 2 days before use in order to ensure its water saturation.

Conclusions

It was shown by FT-ICR MS and MS/MS that pyridine[4]-arene (**C**) forms dimers in the gas phase which may contain guests such as carboxylic acids and amides of different size. Our experiments indicate that these guests are incorporated inside the cavity. This is also true in solution as can be proven by ^{19}F NMR spectroscopy.

Supporting Information Available: Atomic coordinates and pictures (GIF) of the calculated structures **11**−**20**. This material is available free of charge via the Internet at http://pubs.acs.org.

JA049128X